

# Staggered eigenvalue mimicry

Stephan Dürr<sup>a</sup>, Christian Hoelbling<sup>b</sup> and Urs Wenger<sup>c</sup>

<sup>a</sup> DESY Zeuthen, Platanenallee 6, D-15738 Zeuthen, Germany

<sup>b</sup> Centre de Physique Théorique, Case 907, CNRS Luminy, F-13288 Marseille Cedex 9, France

<sup>c</sup> NIC/DESY Zeuthen, Platanenallee 6, D-15738 Zeuthen, Germany

## Abstract

We study the infrared part of the spectrum for UV-filtered staggered Dirac operators and compare them to the overlap counterpart. With sufficient filtering and at small enough lattice spacing the staggered spectra manage to “mimic” the overlap version. They show a 4-fold near-degeneracy, and a clear separation between would-be zero modes and non-zero modes. This suggests an approximate index theorem for filtered staggered fermions and a correct sensitivity to the topology of QCD. Moreover, it supports square-rooting the staggered determinant to obtain dynamical ensembles with  $N_f=2$ .

## 1 Introduction

Recent years have brought a remarkable increase of interest in dynamical ( $N_f=2$  or  $N_f=2+1$ ) QCD runs employing staggered sea-quarks. One of the conceptual issues with these efforts is that the staggered quark action is not doubler-free; a single staggered field will eventually generate four flavors in the continuum. Hence, to create an ensemble with  $N_f=2$ , one simply uses the square-root of the staggered determinant, and for  $N_f=2+1$  an additional quartic-root with a higher mass. The problem is that taking a fractional power of the determinant is, in general, not a legitimate operation in quantum field-theory, contrary to positive integer powers. The worst-case scenario is, therefore, that these runs might not represent an ab-initio approach to QCD in the strong coupling regime. In this respect it does not help that the recent staggered  $N_f=2+1$  results with light sea-quarks look very promising [1]. It has been clearly pointed out by Jansen at the Tsukuba conference [2] and in DeGrand’s review [3] that – if the square-rooting trick cannot be justified – dynamical staggered runs with  $N_f \notin 4\mathbb{N}$  must be considered a *model* of QCD. The results in [1] show that it would be a much better model than quenched QCD, but from a fundamental point of view little is won if the answer would be that there is no justification for the fractional power.

The goal of this note is to confront the low-lying eigenvalues of the massless staggered Dirac operator [4] with analogous spectra of a “benchmark” operator which is known to be without conceptual problems. We choose the massless overlap operator [5], since it satisfies (like domain-wall [6] and classically perfect [7] fermions) the Ginsparg-Wilson relation [8]

$$D\gamma_5 + \gamma_5 D = \frac{1}{\rho} D\gamma_5 D \quad (1)$$

with  $\rho$  a parameter to be specified later. This relation is of prime interest, because it implies invariance of the action (at finite lattice spacing) under the adapted chiral transformation [9]

$$\delta\psi = \gamma_5(1 - \frac{1}{\rho}D)\psi, \quad \delta\bar{\psi} = \bar{\psi}\gamma_5, \quad (2)$$

which in turn excludes additive mass renormalization and prevents operators in different chiral multiplets from mixing. On the other hand, the staggered action breaks the full  $SU(N_f=4)_A$  flavor symmetry, but the remnant  $U(1)$ -symmetry

$$\chi(x) \rightarrow \exp(i\theta_A(-1)^{\sum x_\nu})\chi(x), \quad \bar{\chi}(x) \rightarrow \bar{\chi}(x) \exp(-i\theta_A(-1)^{\sum x_\nu}), \quad (3)$$

still protects the fermion mass against additive renormalization.

A point worth emphasizing is that modern staggered simulations use highly “improved” staggered quarks. These are operators where one replaces in the usual definition

$$D^{\text{stag}} = \frac{1}{2} \sum_{\mu} \eta_{\mu}(x) (U_{\mu}(x)\delta_{x+\hat{\mu},y} - U_{\mu}^{\dagger}(x-\hat{\mu})\delta_{x-\hat{\mu},y}) \quad (4)$$

[with  $\eta_{\mu}(x) = (-1)^{\sum_{\nu < \mu} x_{\nu}}$ ] the parallel transporter  $U_{\mu}(x)$  by a weighted sum of several gauge-covariant paths from  $x$  to  $x+\hat{\mu}$ , and there is an abundance of proposals which terms should enter and what are useful weights [10]. From the Symanzik point of view [11], these actions are in general *not improved* – they are in the same class with  $O(a^2)$  cut-off effects as the original staggered action (albeit the extrapolation slope is typically reduced, and the scaling window might begin earlier). Since these modifications are designed to reduce the dramatic background fluctuations at the cut-off level (in particular the “taste-changing” interactions due to highly virtual gluon exchanges [10]), one should rather speak of “UV-filtered” staggered quarks.

The massless overlap operator is defined through [5]

$$D^{\text{over}} = \rho(1 + D_{-\rho}^{\text{W}}(D_{-\rho}^{\text{W}\dagger}D_{-\rho}^{\text{W}})^{-1/2}) = \rho(1 + \gamma_5 \text{sign}(\gamma_5 D_{-\rho}^{\text{W}})) \quad (5)$$

with  $D_{-\rho}^{\text{W}}$  the Wilson operator at negative mass  $-\rho$ . In the free field limit  $\rho=1$  is appropriate, but for finite  $\beta$  one usually chooses some  $\rho > 1$  to optimize the locality of  $D^{\text{over}}$  [12]. Given the success of the UV-filtered staggered operators, it is natural to consider modified overlap operators where the Wilson Kernel is constructed from smoothed parallel-transporters, too [13, 14]. The resulting filtered overlap operator is still in the Symanzik class with  $O(a^2)$  artefacts, if one stays at a fixed smearing level for all  $\beta$ . In other words: The choice of the covariant derivative in  $D^{\text{W}}$  is an  $O(a^2)$  ambiguity in  $D^{\text{over}}$  like the choice of  $\rho$ . We thus take the liberty to fix  $\rho=1$  at all  $\beta$ -values (except for one check), and to just change the smearing level.

With this setup we are ready for an investigation, which mainly follows the “spectral hint” section of Ref. [14]. To come back to the starting point, what one would like to check is whether UV-filtered staggered quarks develop approximately 4-fold degenerate eigenvalues which coincide with the overlap counterparts such that the rooted staggered determinant generates, up to  $O(a^2)$  cut-off effects, the correct ensemble with 1 or 2 light sea-quarks,

$$\det D^{\text{over}} \propto (\det D^{\text{stag}})^{1/4} + O(a^2). \quad (6)$$

Our approach is to focus on the technically simpler version

$$\det D_{\text{UV-filtered}}^{\text{over}} \propto (\det D_{\text{UV-filtered}}^{\text{stag}})^{1/4} + O(a^2), \quad (7)$$

which is equivalent, since the two left- and the right-hand sides differ by a trivial rescaling and  $O(a^2)$  terms only. If such a relationship can be shown, the overlap operator would be a local operator with the same determinant, up to cut-off effects, as the rooted staggered operator, hence providing a bypass to the locality issue for the valence quarks presented in [15].

## 2 Low-lying eigenvalues of UV-filtered Dirac operators

The plan is to compare – configuration by configuration – the low-lying eigenvalue spectrum of a UV-filtered staggered Dirac operator against that of a filtered overlap operator.

Regarding the filtering, we decided not to follow the details of current state-of-the-art staggered fermions, but to concentrate on two prototype constructs, the APE [16] and HYP [17] smoothed links with the  $SU(3)$ -projection of Ref. [18] which are used for both types of lattice fermions. Throughout, we used the parameters  $\alpha_{\text{APE}}=0.5$  [16] and  $\alpha_{\text{HYP}}=(0.75, 0.6, 0.3)$  [17]. By comparing the two recipes and the various iteration levels, we will be able to judge how much our results are robust against changing the details of the smearing procedure.

The key issue is whether these filtered staggered Dirac operators develop an approximate 4-fold degeneracy, as it has been demonstrated in great detail in 2D (where the degeneracy is 2-fold) [14], and seen more recently in 4D [19].

### 2.1 Dynamical lattices

Let us begin with a full QCD set that was used for spectroscopy. CU\_0001 is an ensemble of 49 configurations with  $16^3 \times 32$  geometry, generated (via the square-root trick) with 2 “tastes” of staggered quarks at bare mass  $m=0.01$  and coupling  $\beta=5.7$ . The lattice spacing is around  $a \simeq 0.1$  fm. We downloaded it from [20], the pertinent original publication is [21].

In order to select configurations with and without overlap zero modes, we first measured a lattice version of the continuum topological charge  $q_{\text{nai}} = \frac{1}{32\pi^2} \sum_x \text{tr}(\epsilon_{\mu\nu\sigma\rho} F_{\mu\nu} F_{\sigma\rho})$ , where  $F_{\mu\nu}$  is defined via the clover-leaf construction involving smeared links (7 HYP steps). Based on this, we selected the configurations shown in Tab. 1 for the spectral analysis. The occurrence of configurations where the overlap index  $n_- - n_+ = \frac{1}{2\rho} \text{tr}(\gamma_5 D^{\text{over}})$  (denoted  $q$  in the following) depends on the smearing level and type (or on the projection parameter  $\rho$ ) is of no concern – it is a typical  $O(a^2)$  effect. The ambiguity is not removed by using vigorously filtered operators, but it disappears in the continuum limit.

Since  $D^{\text{stag}}$  and  $D^{\text{over}}$  are normal, we determined the spectra of the hermitean operators  $D^{\text{stag}\dagger} D^{\text{stag}}$ ,  $D^{\text{over}\dagger} D^{\text{over}}$  and reconstructed the staggered and overlap eigenvalues, respectively. The eigenvalues of the hermitean operators have been determined with the Ritz functional method [22]. We present the eigenvalues of  $D^{\text{stag}}$  and the chirally rotated

$$\hat{\lambda} = \left(1/\lambda - 1/(2\rho)\right)^{-1} \quad (8)$$

of  $D^{\text{over}}$  which are both purely imaginary. Figs. 1, 2, 3 contain our results. The thin-link operators are compared on the left-most side, and the filtered cousins with the same type of parallel-transporters are arranged next to each other. With  $a^{-1} \simeq 2$  GeV the energy axis includes modes up to 160 MeV.

|                |          |          |         |                     |
|----------------|----------|----------|---------|---------------------|
| u_CU_0001.0500 | conf_000 | 0.577307 | +0.9469 | +1                  |
| u_CU_0001.1200 | conf_006 | 0.577942 | -1.8857 | -2                  |
| u_CU_0001.2000 | conf_014 | 0.577612 | +0.0248 | (-1, -1, +1, 0, +1) |
| u_CU_0001.3200 | conf_026 | 0.577187 | -0.0981 | 0                   |
| u_CU_0001.4400 | conf_038 | 0.577232 | +0.8983 | (+1, +1, +1, 0, +1) |
| u_CU_0001.5400 | conf_048 | 0.577220 | -4.4203 | -5                  |

Table 1: Original name, nickname, plaquette,  $q_{\text{nai}}$  and  $n_- - n_+$  of the CU\_0001 configurations. Whenever they would not agree the indices for the standard, 1 APE, 3 APE, 1 HYP and 3 HYP overlap operators are given separately.

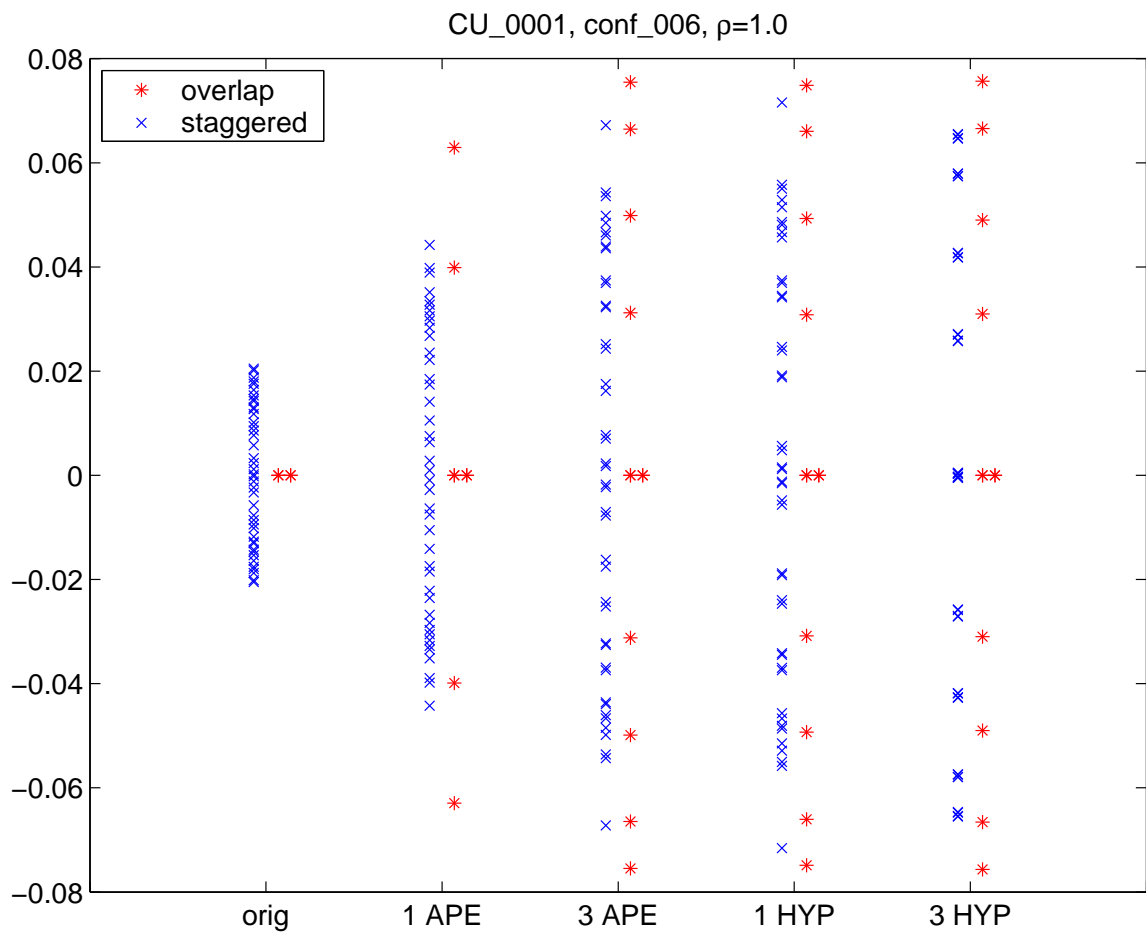
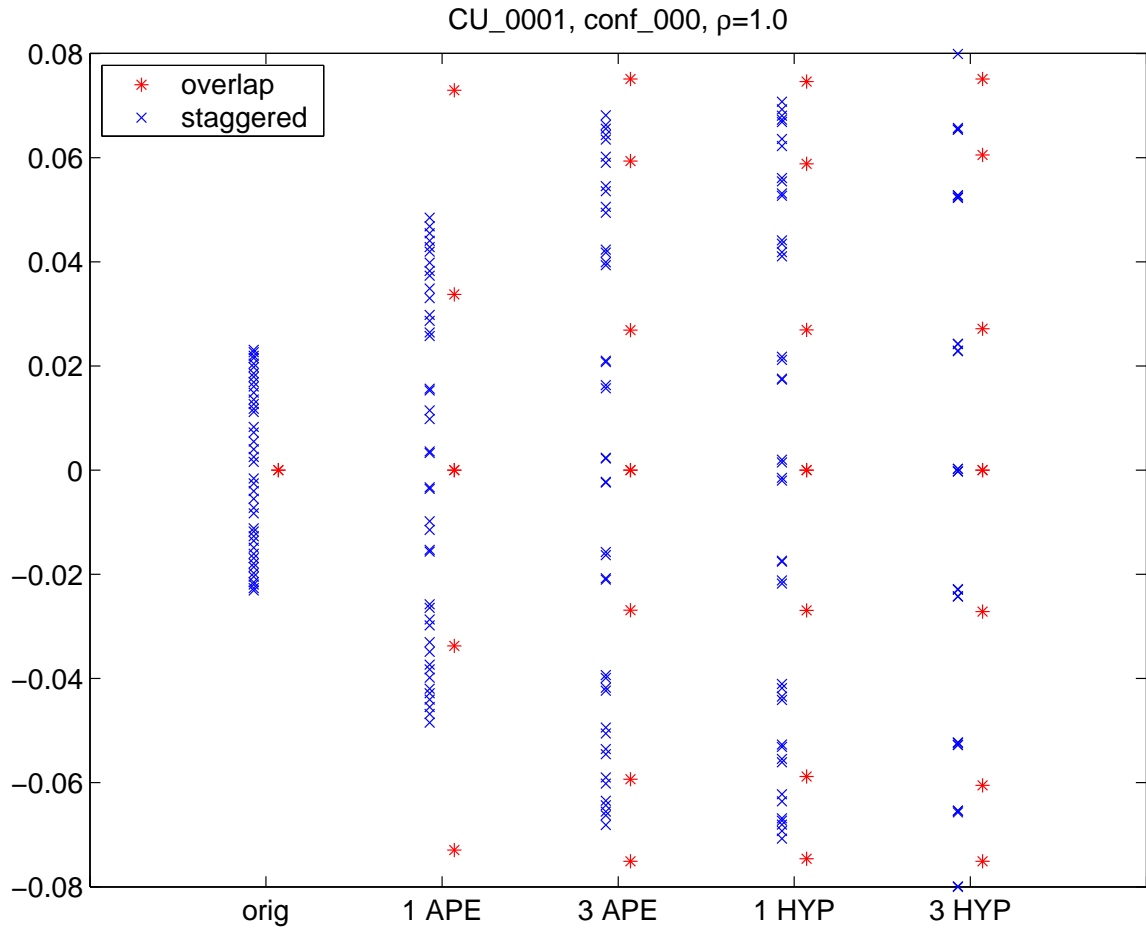


Figure 1: Eigenvalues on the configurations 00 and 06 in the ensemble CU\_0001.

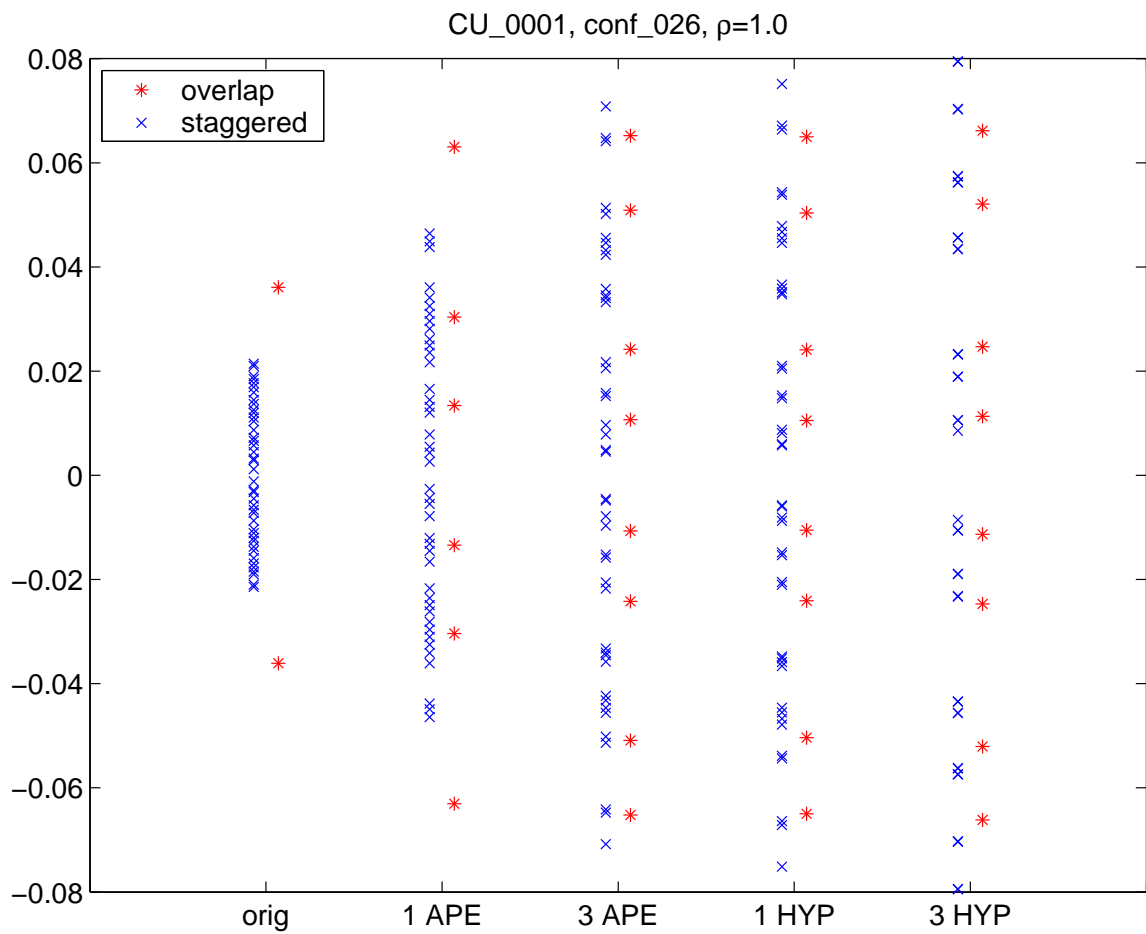
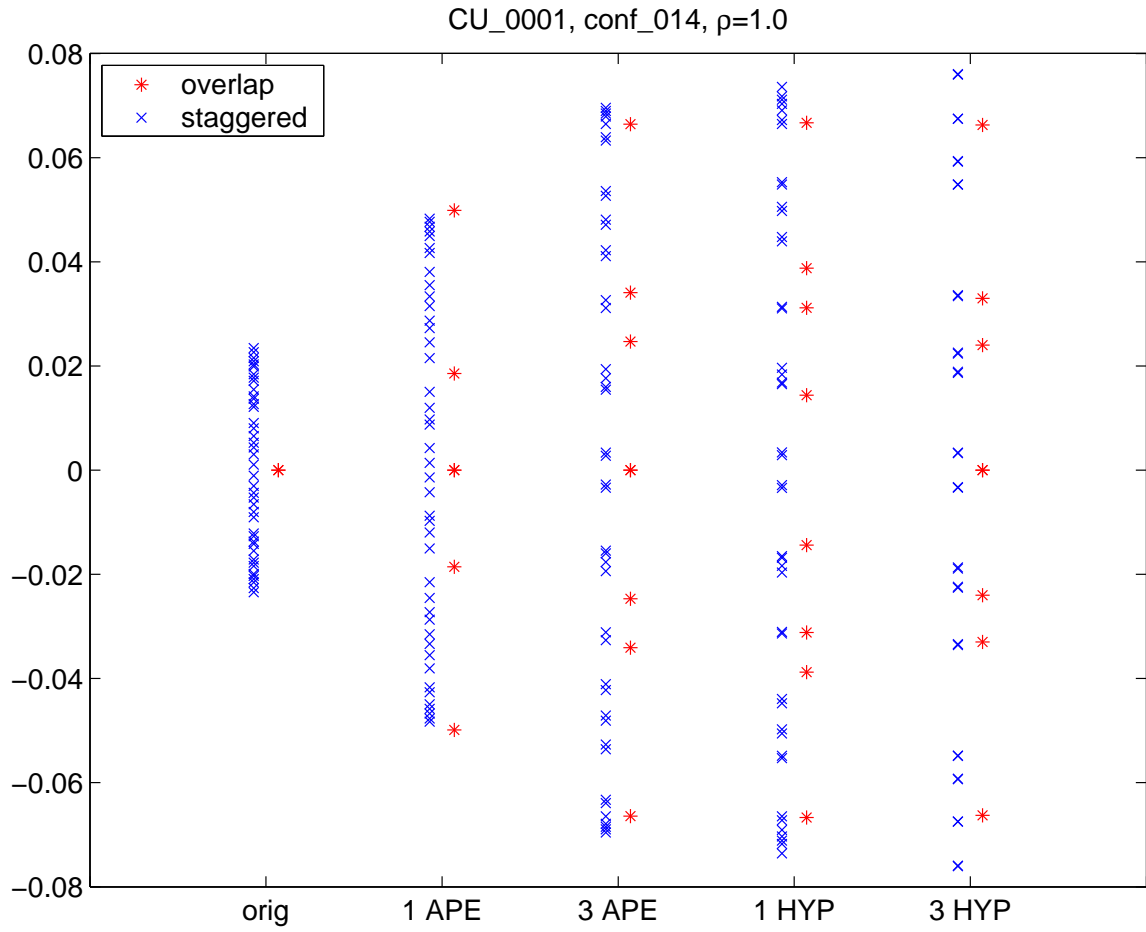


Figure 2: Eigenvalues on the configurations 14 and 26 in the ensemble CU\_0001.

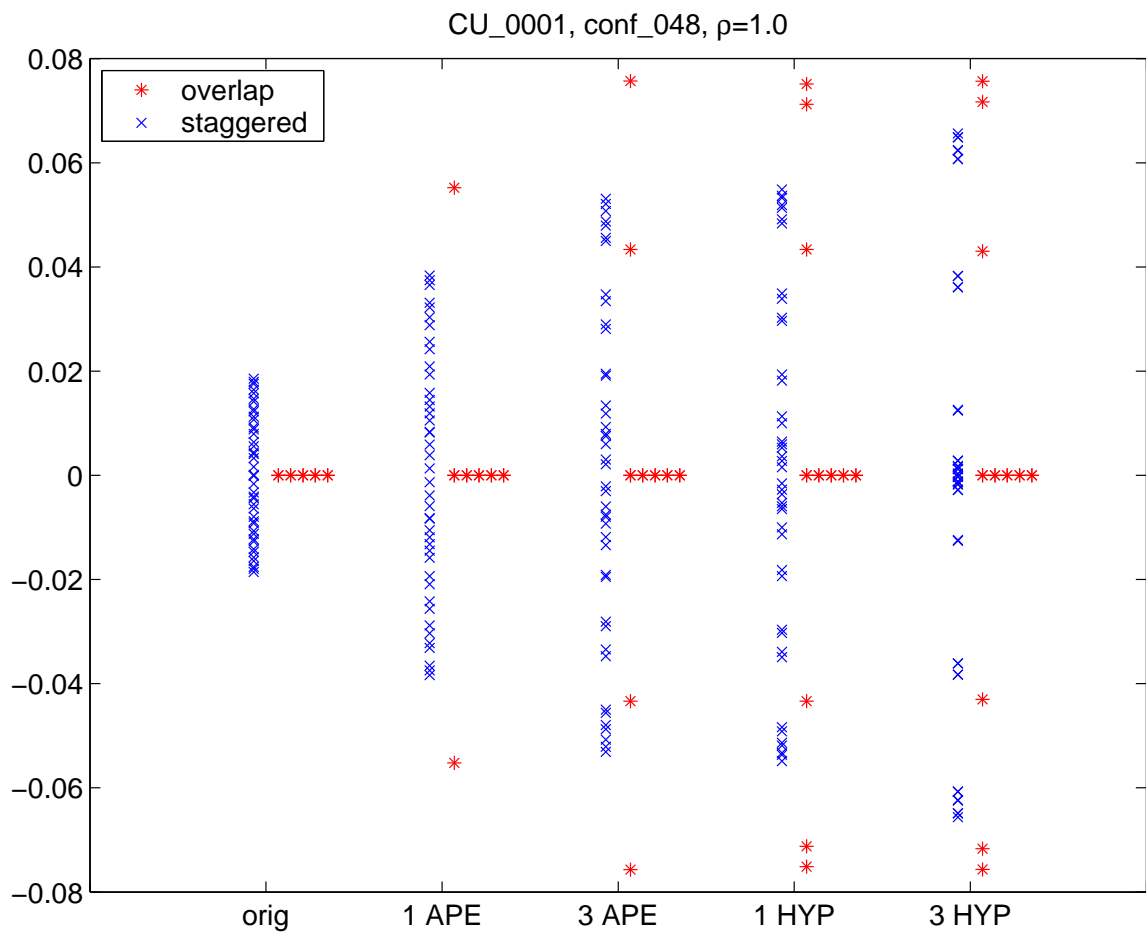
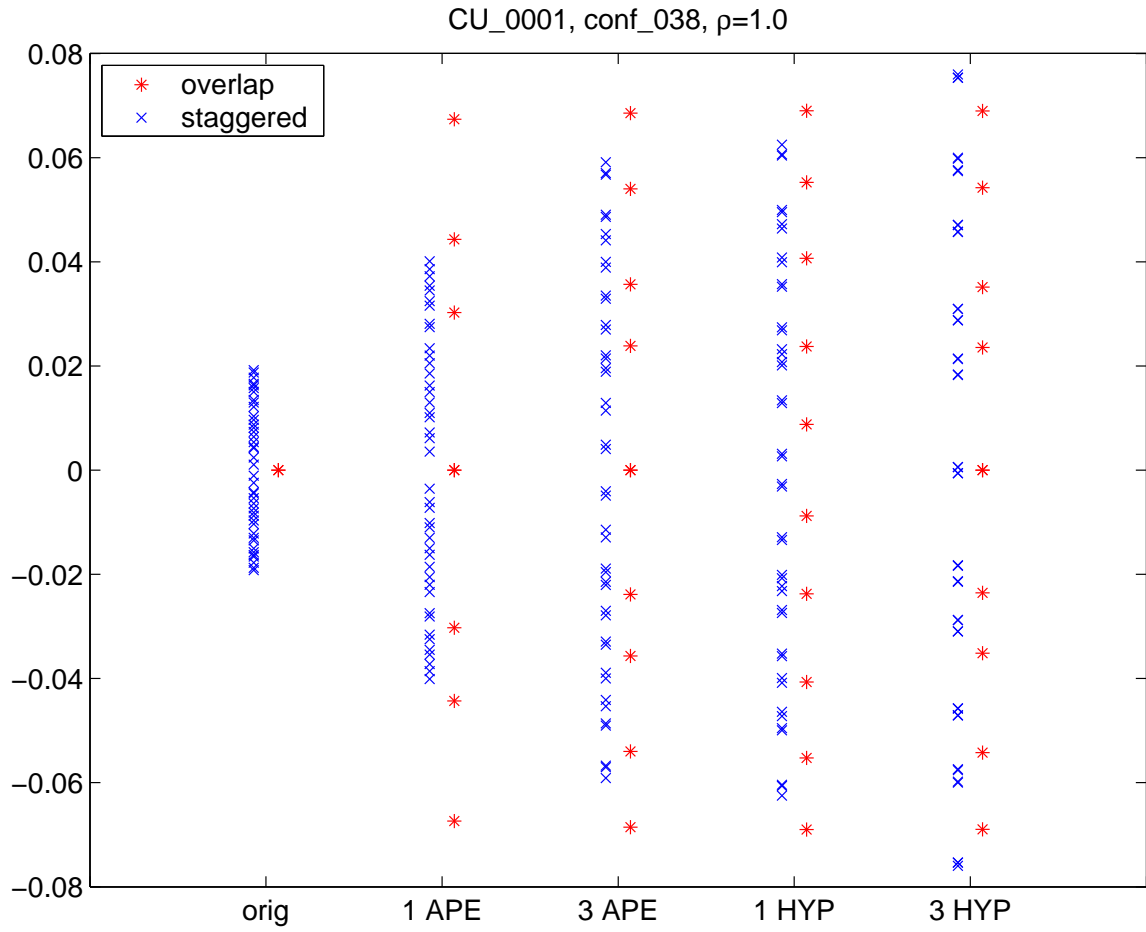


Figure 3: Eigenvalues on the configuration 38 and 48 in the ensemble CU\_0001.

The original operators show no similarity at all. Upon employing one APE-smearing step, the staggered spectra get stretched while the overlap-spectra get squeezed. Still, there is no similarity, but the *eigenvalue densities* (divided by 4 in the staggered case) have been equalized quite a bit. At intermediate filtering levels (3 APE and 1 HYP steps) all staggered eigenvalues have grouped into almost-degenerate twin-pairs. At the 3 HYP level, finally, a second grouping of twin-pairs into *quadruples of near-degenerate staggered eigenmodes* has taken place. Stretching the staggered 3 HYP spectra with a factor  $Z \simeq 1.2$ , one finds a rather convincing agreement between the quadruples and the (individual) overlap modes. There is a clear *gap* between staggered “would-be” zero modes and non-zero modes, though this rule is challenged by some configurations. On conf\_014 (and to some extent on conf\_038) the operator  $D_{3\text{HYP}}^{\text{stag}}$  reproduces the confusion that the overlap has regarding the charge of this configuration (cf. footnote 1). And conf\_048 seems to be hard to resolve, simply for its high  $|q|$ . Note, finally, the stability (on a clear majority of configurations) of the low-lying overlap spectrum from 3 APE through 3 HYP.

All these findings are in complete analogy to what has been seen in great detail in 2D [14]. The only difference is that the near-degeneracy is 2-fold there, since (3) is the lattice remnant of the  $SU(N_f=2)$  symmetry in 2D.

## 2.2 Matched quenched lattices

To check whether  $O(a^2)$  effects really capture the difference between filtered staggered and overlap spectra, we generated 4 sets of matched quenched lattices, aiming at  $L/r_0 = 2.24$  with the Sommer scale  $r_0 \simeq 0.5 \text{ fm}$  [23]. In a physical volume  $V \simeq (1.12 \text{ fm})^4 \simeq 1.57 \text{ fm}^4$  there are finite volume effects, but we expect them not to spoil the spectral analogy, if it emerges at the given coupling. Using the interpolation formula in [24] for the Wilson gauge action, one finds that the pairs  $(L=6, \beta=5.66)$ ,  $(L=8, \beta=5.79)$ ,  $(L=12, \beta=6.0)$ ,  $(L=16, \beta=6.18)$  produce the desired volume (the first coupling is slightly out of bound, the formula holds for  $5.7 \leq \beta \leq 6.57$ ).

Tables 2-5 contain the absolute values of the overlap indices on our  $6^4, 8^4, 12^4, 16^4$  lattices. As expected, the fraction of configurations on which the 1 APE, 3 APE, 1 HYP and 3 HYP overlap operators agree on the charge increases with  $\beta$  (for  $\beta \rightarrow \infty$ , this fraction is one). Table 2 is interesting in another respect: The normal “rule” (at high  $\beta$ ) that additional smearing operations will reduce the charge (here, we ignore the unsmear column) is broken at low  $\beta$  (at  $\beta=5.66$  there are five such configurations). Finally, Table 3 also contains our test regarding the impact of the projection parameter  $\rho$  in (5). On the first configuration, besides using  $\rho=1$ , we determined the spectrum with  $\rho=1.6$ . The standard and 1 APE overlap operators prove sensitive to this shift, the more vigorously filtered versions not. This is fully compatible with the view that the charge ambiguity is an  $O(a^2)$  effect; with strong UV-filtering the coefficient in front of the artefact gets smaller. Interestingly,  $D_{63\text{APE}, 63\text{HYP}}^{\text{over}}$  still yield reasonable charge determinations, in spite of these operators being entirely non-local on our small lattices.

We tested on the  $8^4$  configurations whether the  $SU(3)$ -projection in the APE [16] or HYP [17] smearing recipes could be skipped. The answer is negative: With one smearing step, the impact is not so dramatic, but after two more the staggered spectra are dramatically squeezed (rather than stretched out), so that there is no agreement with the (filtered and projected) overlap spectrum at all.

Contrary to the CU\_0001 case, we refrain from showing all spectra. For the lack of a good criterion, we simply select the first configuration of our  $6^4, 8^4, 12^4, 16^4$  chains, respectively. In Figures 4 and 5 the (ordered) staggered eigenvalues (with projection) are plotted against their serial number. One clearly observes how the expected 4-fold near-degeneracy gets more

| $\beta=5.66$ | 1 APE | 3 APE | 7 APE | 63 APE | 1 HYP | 3 HYP | 7 HYP | 63 HYP |
|--------------|-------|-------|-------|--------|-------|-------|-------|--------|
| 000          | 1     | 2     | 1     | 1      | 2     | 1     | 1     | 1      |
| 001          | 1     | 1     | 1     | 0      | 2     | 1     | 1     | 0      |
| 002          | 1     | 1     | 2     | 1      | 2     | 2     | 2     | 1      |
| 003          | 0     | 0     | 0     | 1      | 0     | 0     | 0     | 0      |
| 004          | 0     | 1     | 1     | 2      | 1     | 2     | 2     | 2      |
| 005          | 1     | 1     | 0     | 0      | 1     | 0     | 0     | 0      |
| 006          | 1     | 2     | 2     | 2      | 2     | 2     | 2     | 2      |
| 007          | 1     | 1     | 1     | 1      | 1     | 1     | 1     | 1      |
| 008          | 0     | 0     | 0     | 0      | 0     | 0     | 0     | 0      |
| 009          | 0     | 0     | 0     | 0      | 0     | 0     | 0     | 0      |

Table 2: Number of zero modes of various overlap operators on our quenched  $6^4$  configurations. The 1 APE, 3 APE, 1 HYP and 3 HYP operators agree for 4 of the 10 configurations.

| $\beta=5.79$ | orig | 1 APE | 3 APE | 7 APE | 1 HYP | 3 HYP | 7 HYP |
|--------------|------|-------|-------|-------|-------|-------|-------|
| 000          | 1(2) | 2(3)  | 2(2)  | 2(2)  | 2(2)  | 2(2)  | 2(2)  |
| 001          | 1    | 1     | 1     | 1     | 1     | 1     | 1     |
| 002          | 0    | 1     | 0     | 1     | 1     | 1     | 1     |
| 003          | 1    | 2     | 2     | 2     | 2     | 2     | 2     |
| 004          | 0    | 1     | 1     | 1     | 1     | 1     | 1     |
| 005          | 0    | 0     | 0     | 0     | 0     | 0     | 0     |

Table 3: Number of zero modes of various overlap operators on our quenched  $8^4$  configurations. On the first configuration, the values for  $\rho = 1.6$  are in brackets. The 1 APE, 3 APE, 1 HYP and 3 HYP operators agree for 5 of the 6 configurations.

| $\beta=6.0$ | orig | 1 APE | 3 APE | 7 APE | 1 HYP | 3 HYP | 7 HYP |
|-------------|------|-------|-------|-------|-------|-------|-------|
| 000         | 1    | 1     | 1     | 1     | 1     | 1     | 1     |
| 001         | 0    | 0     | 0     | 0     | 0     | 0     | 0     |
| 002         | 1    | 1     | 1     | 1     | 1     | 1     | 1     |
| 003         | 0    | 0     | 0     | 0     | 0     | 0     | 0     |
| 004         | 1    | 1     | 1     | 1     | 1     | 1     | 1     |
| 005         | 1    | 1     | 1     | 1     | 1     | 1     | 1     |

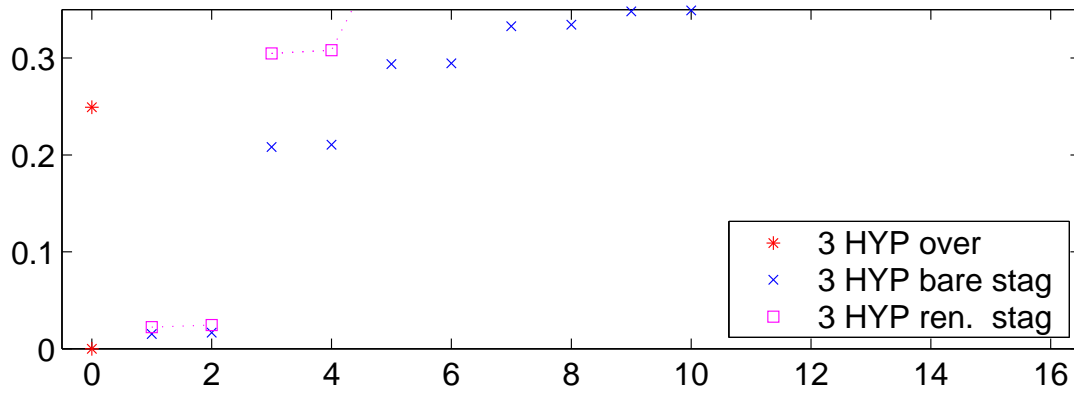
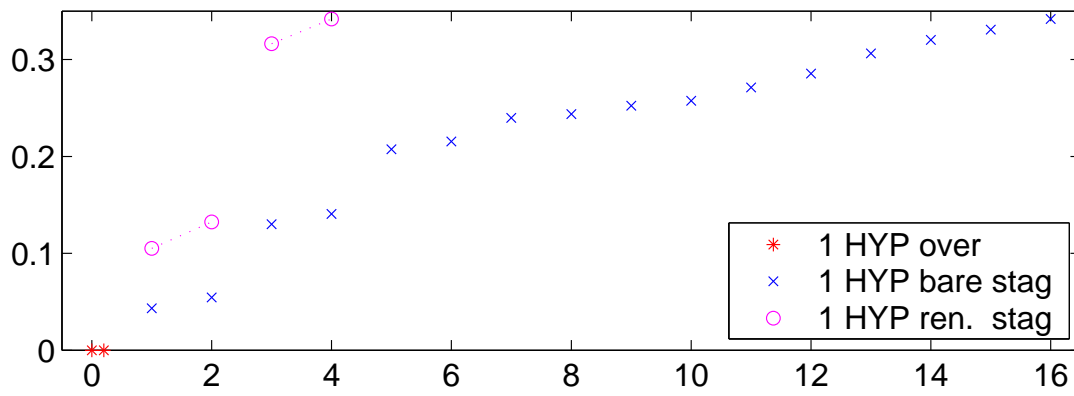
Table 4: Number of zero modes of various overlap operators on our quenched  $12^4$  configurations. The 1 APE, 3 APE, 1 HYP and 3 HYP operators agree for all 6 configurations.

| $\beta=6.18$ | orig | 1 APE | 3 APE | 7 APE | 1 HYP | 3 HYP | 7 HYP |
|--------------|------|-------|-------|-------|-------|-------|-------|
| 000          | 0    | 0     | 0     | 0     | 0     | 0     | 0     |
| 002          | 0    | —     | —     | —     | 0     | 0     | 0     |
| 004          | 0    | 0     | 0     | 0     | 0     | 0     | 0     |
| 006          | 0    | —     | —     | —     | 0     | 0     | 0     |
| 008          | 1    | 1     | 1     | 1     | 1     | 1     | 1     |
| 010          | 1    | —     | —     | —     | 2     | 2     | 1     |
| 012          | 1    | 1     | 1     | 1     | 1     | 1     | 1     |
| 014          | 1    | —     | —     | —     | 1     | 1     | 1     |
| 016          | 1    | —     | —     | —     | 1     | 1     | 1     |

Table 5: Number of zero modes of various overlap operators on our quenched  $16^4$  configurations. The 1 APE, 3 APE, 1 HYP and 3 HYP operators agree for all 4 configurations on which they have all been determined.



$6^4$ ,  $\beta=5.66$ , conf\_000,  $\rho=1.0$



$8^4$ ,  $\beta=5.79$ , conf\_000,  $\rho=1.0$

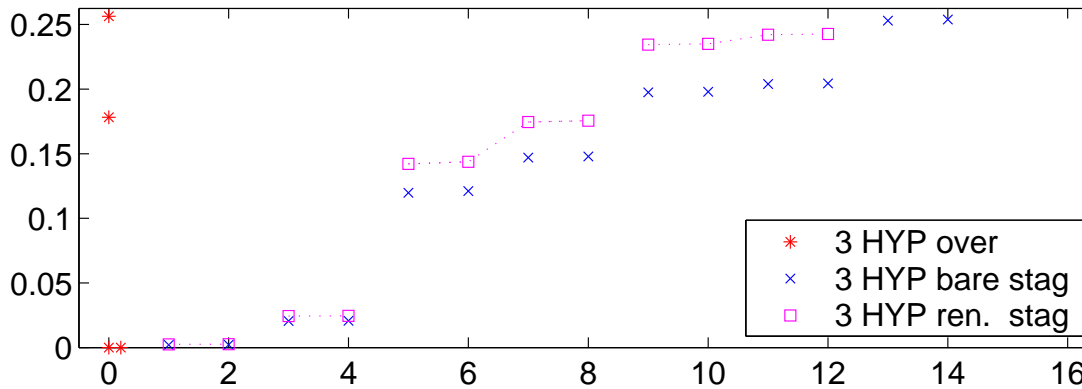
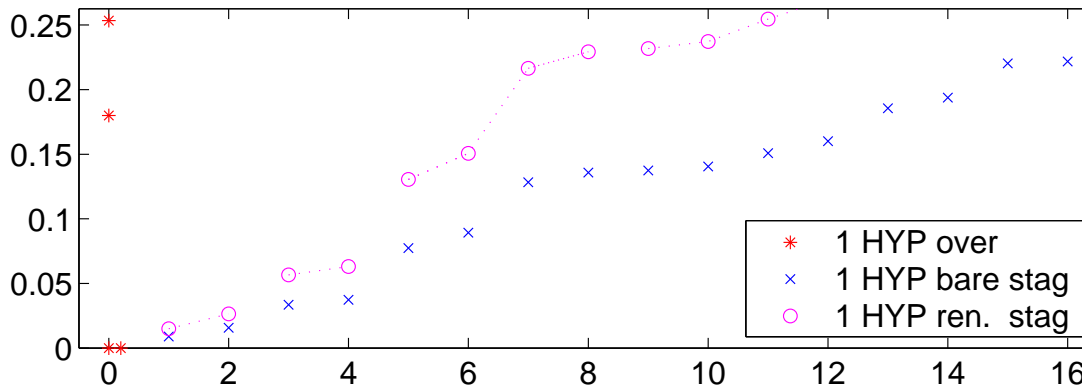


Figure 4: Staggered eigenvalues with/without relative normalization factor on the first one of our  $6^4$  and  $8^4$  lattices, compared to the corresponding overlap spectrum.

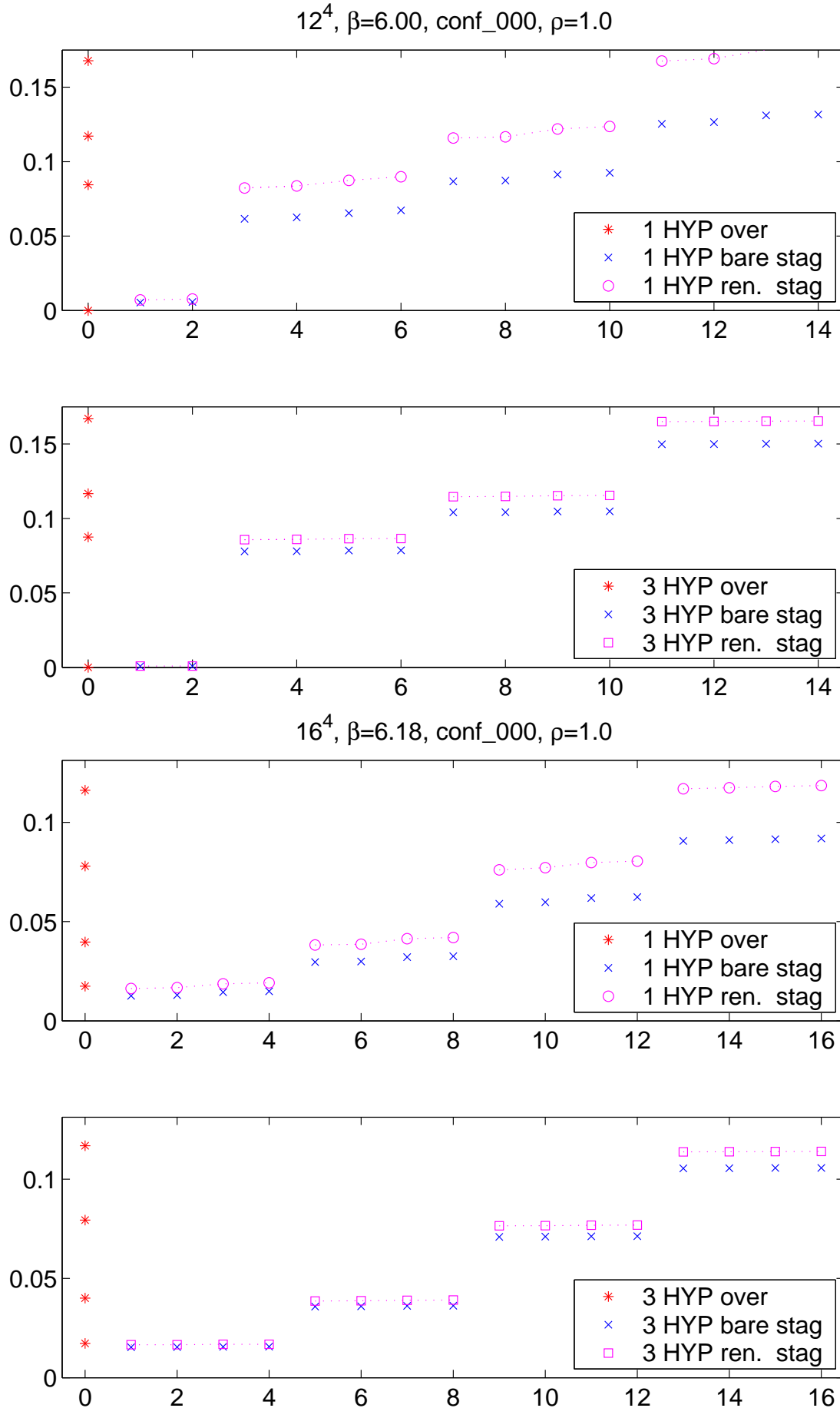


Figure 5: Staggered eigenvalues with/without relative normalization factor on the first one of our  $12^4, 16^4$  lattices, compared to the corresponding overlap spectrum.

pronounced as  $\beta$  increases; at  $\beta=6.18$  there is a clear “terrace dynamics”. This picture holds for  $D_{1\text{HYP}}^{\text{stag}}$ , and for  $D_{3\text{HYP}}^{\text{stag}}$  it is even more convincing. On the left, the IR-spectrum of the overlap operator with the same type of filtering is shown. Finally, the appropriate relative normalization factor (slope in Figs. 6 and 7, see below) is applied to the staggered spectrum to make it a fair comparison. The bottom line is that, at sufficiently weak coupling, it is appropriate to identify the *geometric mean of a near-degenerate quadruple* with a single *eigenvalue* of the overlap operator. Whether there is, in addition, a relationship between the modes – ideally, one would like to give a construction which, in analogy to the one by Kogut and Susskind, manages to (approximately) *thin out the degrees of freedom* – is a challenge for the future.

Our Figures 4 and 5 cover a fixed energy range up to  $\sim 370$  MeV. They demonstrate that both the separation between would-be zero modes and non-zero modes and the grouping into quadruples crucially depend on the lattice spacing – below  $a^{-1} \simeq 2$  GeV even a high level of filtering does not help. And, by comparing to the filtered overlap we see a *quantitative agreement* for  $a^{-1} > 2 - 2.5$  GeV.

### 2.3 Correlation between staggered and overlap eigenvalues

To check whether the quartic-rooted filtered staggered operator really reproduces the spectrum of the filtered overlap one may plot them, eigenvalue by eigenvalue, against each other.

Restricting ourselves to the positive half of the spectrum, we group the staggered eigenvalues into two classes: The would-be zero modes (we name them  $0 < \zeta_1 < \zeta_2 < \dots$ ) and the (true) non-zero modes (denoted by  $\lambda_1 < \lambda_2 < \dots$  with  $\zeta_{\max=2|q|} < \lambda_1$ ). For the  $n$ -th would-be zero mode we take  $\sqrt{\zeta_{2n-1}\zeta_{2n}}$ , since  $(-\zeta_2, -\zeta_1, \zeta_1, \zeta_2)$  is the substitute of the first zero mode. The  $m$ -th non-zero mode is associated with  $(\lambda_{4m-3} \cdot \dots \cdot \lambda_{4m})^{1/4}$ . This classification is a strict function of  $q$  determined via the overlap against which one compares.

These geometric means are then plotted against the overlap eigenvalues  $\hat{\lambda}$ , results being shown in Figs. 6-7. Here, every symbol corresponds to an individual configuration.

What one sees immediately, is that the agreement gets much better with increasing  $\beta$ . In three graphs there is a “pile” of would-be zero modes above the origin. These are classified so, because the overlap finds a non-zero index, but then they happen to be not-so-small. Since the overlap operator itself has an  $O(a^2)$  ambiguity<sup>1</sup>, this phenomenon is expected to become rare at weak coupling. Unfortunately, even at  $\beta=6.18$  we have one configuration with such a charge ambiguity. The pile also shows up when one overlap is plotted versus another one, say  $D_{1\text{HYP}}^{\text{over}}$  vs.  $D_{7\text{HYP}}^{\text{over}}$ . On the other hand, the fact that one configuration in the  $\beta=6.0$  ensemble goes astray is due to UV-noise which does not affect the charge. One learns that at this coupling even the 1 HYP operator suffers from large UV-fluctuations in its IR-spectrum.

Switching in Figs. 6, 7 from the 1 HYP level (black) to 7 HYP staggered vs. 7 HYP overlap (light), the correlation gets tighter and the relative normalization factor  $Z$  moves closer to 1. Increasing, on the staggered side, the smearing level to 7 HYP, but staying, on the overlap side, at 1 HYP (i.e.  $D_{7\text{HYP}}^{\text{stag}}$  vs.  $D_{1\text{HYP}}^{\text{over}}$ ), the  $Z$ -factor still moves towards 1, but the correlation does *not improve* (not shown). We plan to check that the tight correlation between the lowest eigenmodes extends to the whole determinant, i.e. to verify eqns. (6, 7) directly.

Once  $\beta$  is so large that the pile of not-so-small would-be zero modes is gone and a clear gap to the non-zero modes is observed (cf. Fig. 7), the filtered staggered fermions will satisfy an *approximate index theorem*. This has been demonstrated in great detail in 2D [14], and Refs. [25, 19] have added evidence that this holds in 4D, too.

<sup>1</sup>With another  $\rho$  or an alternative smearing level a different number of staggered modes might have been identified as would-be zero modes.

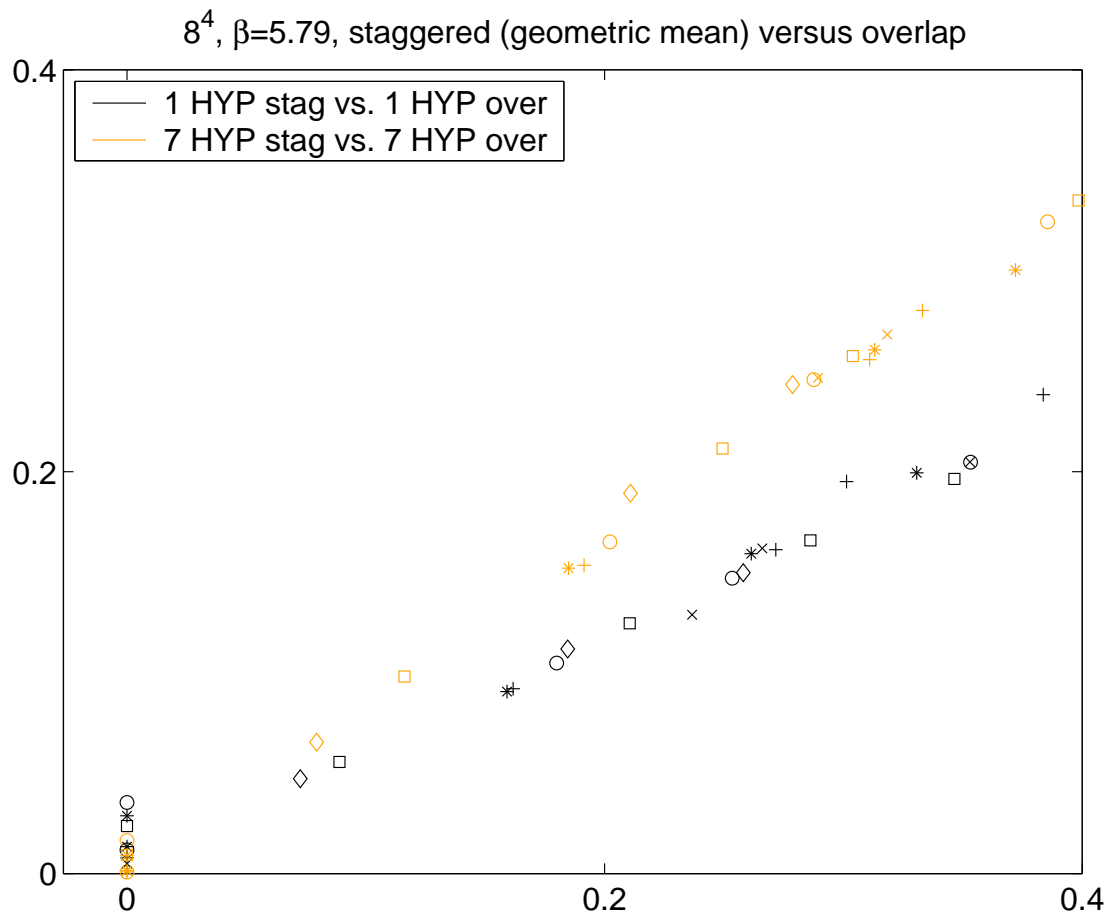
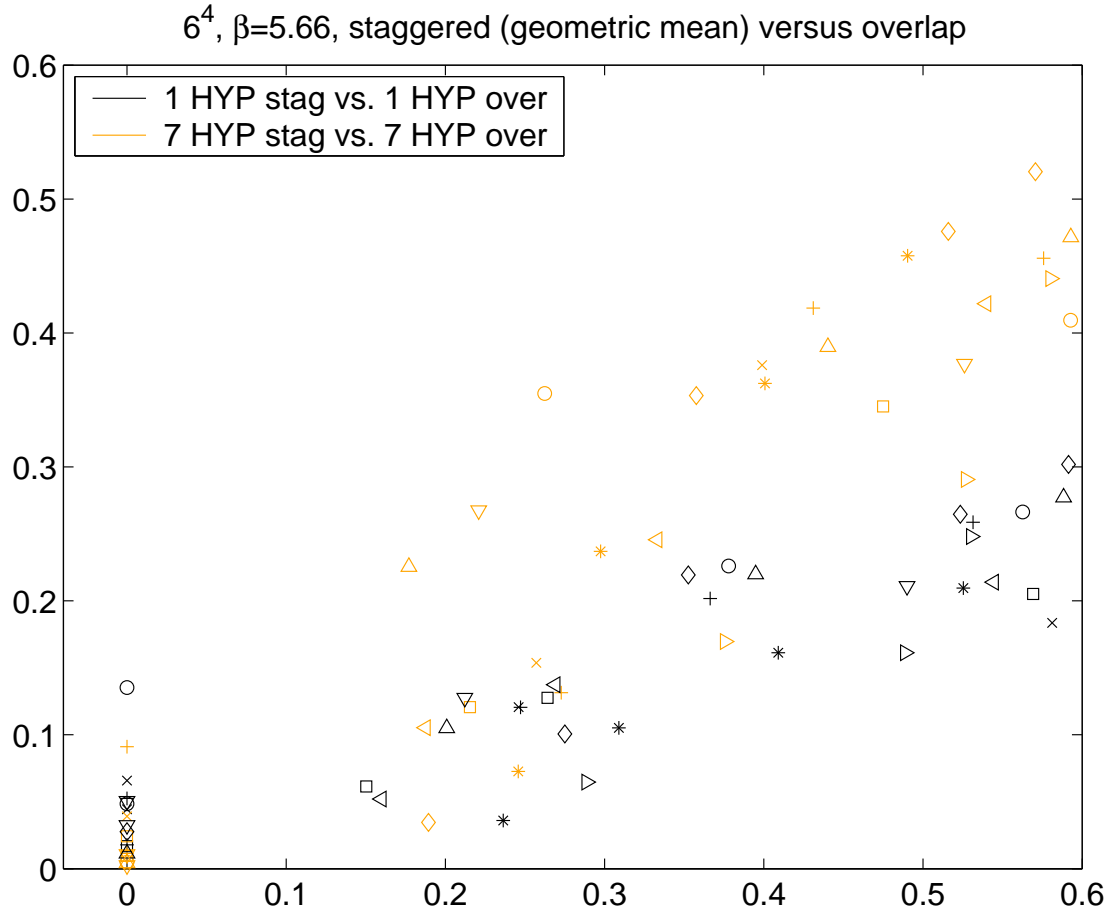


Figure 6: Quartic-rooted staggered versus overlap modes at  $\beta = 5.66$  and  $\beta = 5.79$ . Different symbols refer to different configurations.

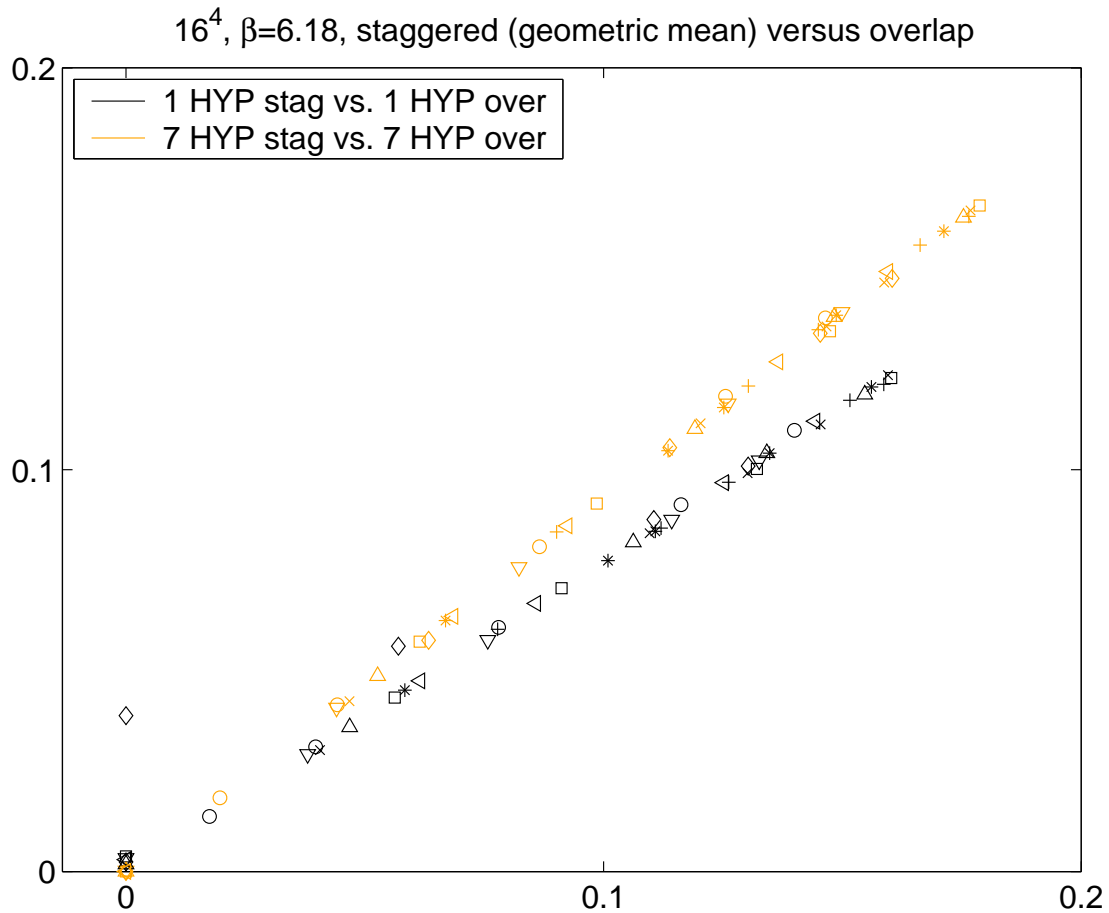
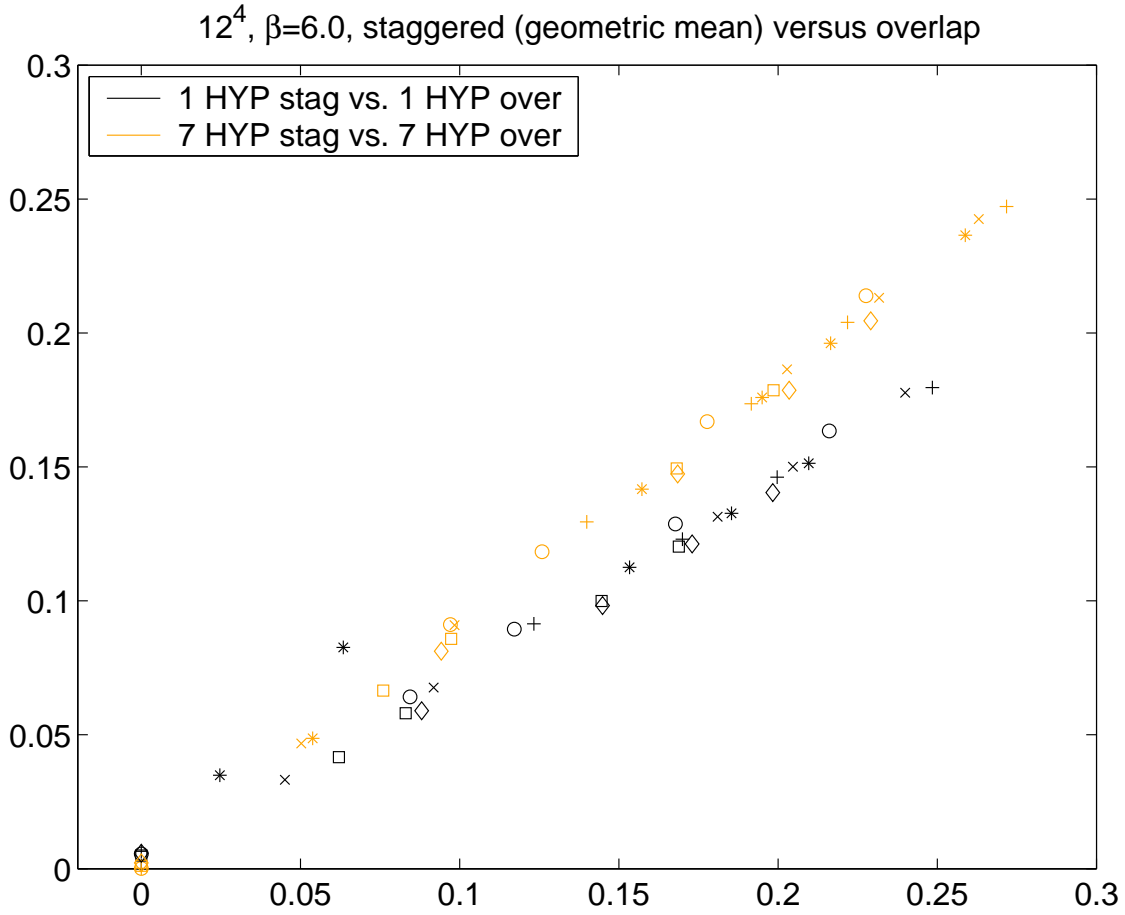


Figure 7: Quartic-rooted staggered versus overlap modes at  $\beta = 6.0$  and  $\beta = 6.18$ . Different symbols refer to different configurations.

Last but not least, the mode-by-mode correspondence implies that (filtered) staggered fermions on sufficiently fine lattices reach agreement with the prediction of random matrix theory, as it has been observed for overlap fermions [26].

## 2.4 Scaling analysis for eigenvalue-splitting pseudo-observables

To define the fuzziness of the lowest would-be zero mode (if present) we form

$$\Delta_0 = \frac{\sqrt{\zeta_2 \zeta_1}}{(\lambda_4 \lambda_3 \lambda_2 \lambda_1)^{1/4} - \sqrt{\zeta_2 \zeta_1}}. \quad (9)$$

To define the fuzziness of the first (true) non-zero mode we construct

$$\Delta_1 = \frac{\sqrt{\lambda_4 \lambda_3} - \sqrt{\lambda_2 \lambda_1}}{(\lambda_8 \lambda_7 \lambda_6 \lambda_5)^{1/4} - (\lambda_4 \lambda_3 \lambda_2 \lambda_1)^{1/4}}. \quad (10)$$

These expressions quantify the non-degeneracy of a quadruple on the scale of its distance to the next one, and tend to zero if the four-fold degeneracy becomes exact.

If the non-degeneracy of the staggered eigenmodes and the fuzziness of the would-be zero modes are just  $O(a^2)$  artefacts (though, numerically, they may be so dramatic that without UV-filtering not even the faintest analogy is seen at accessible couplings), one would expect that the pseudo-observables (10) and (9) vanish (asymptotically) in proportion to  $a^2$ .

Fig. 8 contains our results for the  $8^4$ ,  $12^4$ , and  $16^4$  lattices (the points for the  $6^4$  geometry were omitted since they are definitely not in the scaling regime). Given the smallness of our samples, we have opted for the median instead of the arithmetic mean – this estimator is biased, but far more robust against outliers. Indeed, the 1HYP and 3HYP data seem to be consistent with the hypothesis of asymptotic scaling – although our data do, of course, not pin down the exponent. A linear fit (versus  $a^2$ ) through the  $L = 16, 12$  points (constrained to go through 0, i.e. with 1 d.o.f.) yields an acceptable  $\chi^2$ , and its extension to the right seems compatible with the  $L = 8$  data. On the other hand, the unfiltered data are essentially flat, and there is no way to fit them in this manner. This is precisely the scenario mentioned in the introduction. While we have no doubts that – moving to much weaker couplings – even the unsmearred staggered operator’s pseudo-observables  $\Delta_{0,1}$  would eventually turn down and reach the origin linearly, the big difference with the 1HYP and 3HYP versions is that this happens at *accessible couplings*.

Furthermore, the lesson from 2D is that a typical  $\sqrt{\zeta_{2q} \zeta_{2q-1}}$  of the massless operator gives a reliable estimate down to which quark mass the massive staggered Dirac operator yields trustworthy results [14].

## 2.5 Technical bonus

It is interesting to note that the construction of the UV-filtered overlap operator is much cheaper than the standard version. For the unsmearred CU configurations the condition number of  $H^2 = (\gamma_5 D_{-1}^W)^2$  was in the range  $10^4 - 10^8$ . After projecting out the 11 lowest eigenmodes, this figure gets reduced to  $\sim 350 - 450$ , and the degree of the associate Chebychev polynomial is  $\sim 400$ . After 3HYP steps, the condition number is  $\sim 140 - 15'000$  and  $\sim 60 - 100$ , before and after projection, respectively, and the required degree of the Chebychev polynomial on the subspace orthogonal to the 11 lowest modes is  $\sim 60$ .

Note that this impact on the degree of the polynomial is seen after the lowest 11 eigenvectors have been projected out. This strengthens the impression that one gets from comparing Fig. 2

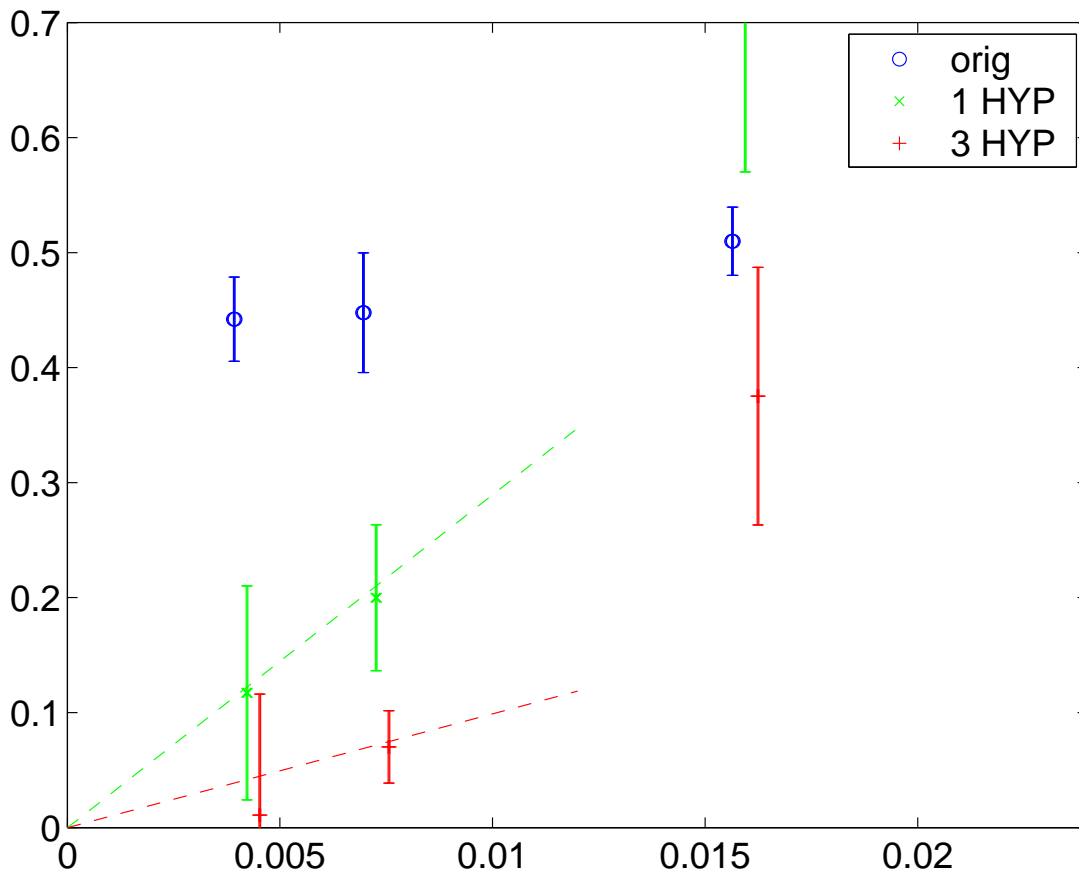
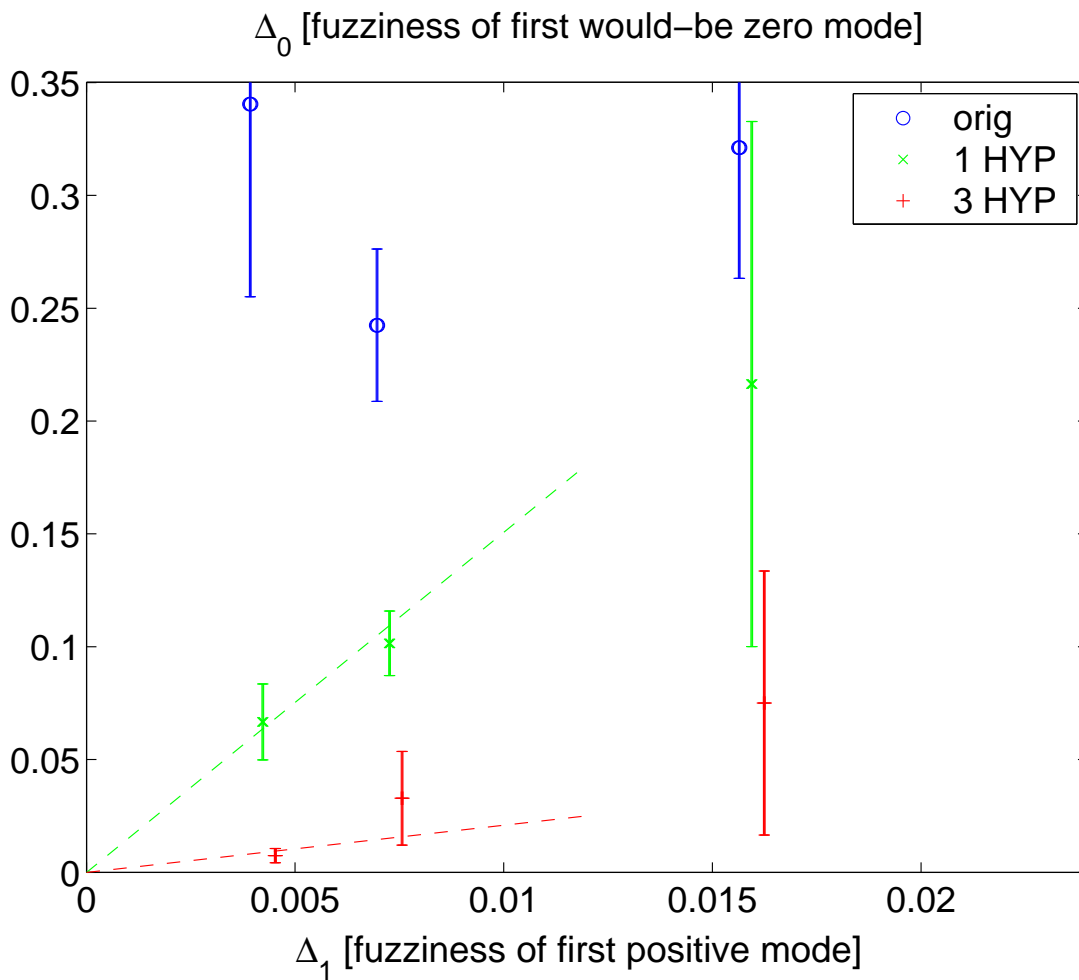


Figure 8: Pseudo-observables  $\Delta_0$  and  $\Delta_1$  vs.  $1/L^2$  for the matched  $8^4, 12^4, 16^4$  lattices.

in Ref. [27] to Fig. 3 in Ref. [28]. In the latter case, the standard (unfiltered) Wilson kernel is evaluated on pure gauge backgrounds generated with the Iwasaki/DBW2 action, and the lowest eigenvalues of  $H^2$  get considerably lifted compared to the Wilson gauge action case. However, after a fixed number of eigenmodes have been projected out, this advantage is considerably reduced (see Fig. 3 of Ref. [28]), since the bulk part of the spectrum is less sensitive to the improvement coefficient than the bottom end of the eigenvalue distribution. In Ref. [27] the fermion action is changed, and this has a huge impact even after a fixed number of eigenvectors is projected out. In line with this, we observe that the *bulk* of the eigenmodes of  $H^2$  for a HYP smeared gauge configuration (which we see as a filtered fermion on the original background) starts at significantly higher values. This holds, regardless whether this configuration was produced with the Wilson gauge action or stems from a full QCD ensemble. Therefore, the construction of the overlap operator with a UV-filtered kernel is considerably cheaper than for a standard Wilson kernel even after projecting out the few lowest eigenmodes of  $H^2$ .

### 3 Summary and Outlook

We have studied a class of UV-filtered staggered and overlap operators that are built with standard techniques, comparing the IR-part of their spectra with and without filtering. We close with a summary of our findings and a few comments on their implications.

1. With sufficient filtering and on fine enough lattices, the staggered fermions develop an ability to separate would-be zero modes from non-zero modes, and arrange them in near-degenerate groups of 4. The second point is that both the number of zero-modes and the quadruples reproduce, up to  $O(a^2)$  effects, the findings of the filtered overlap operator. This implies an approximate index theorem for filtered staggered quarks.
2. For both aspects, the “critical” coupling is (in quenched Wilson terms) around  $\beta_W = 6.0$ . Below, the agreement vanishes rapidly, and there is no way to compensate for this by resorting to higher smearing levels.
3. The agreement, at the level of a single configuration, with the low-energy spectrum of the overlap operator implies that UV-filtered staggered fermions will eventually reproduce the correct random-matrix-theory universality class and the correct continuum limit of topological susceptibility and associate flavor-singlet observables, as a corollary.
4. A rudimentary scaling analysis of two pseudo-observables designed to capture the fuzziness of the staggered would-be zero modes and non-zero modes, respectively, suggests that our data are consistent with the hypothesis that these staggered artefacts vanish like  $O(a^2)$ . This, together with the quantitative agreement with the corresponding overlap eigenvalues, forms evidence in favor of using the fractional power (7) of the filtered staggered determinant.
5. An observation important for quenched overlap spectroscopy is that the filtered overlap is much cheaper than the unfiltered one. This is a distinctive feature of the kernel in (5), and not tied to any particular action used to generate the background.
6. Our line-up and correlation plots at weak coupling (Figs. 5 and 7) bear the promise to trigger a new development in lattice QCD. With such an excellent one-to-four agreement of the low-lying spectra, it might be possible to run a dynamical  $N_f = 2$  staggered simulation, performing the final accept/reject-step with the overlap action (or, alternatively,



to reweight the ensemble to  $N_f = 2$  overlap flavors). In other words, the perspective is to perform a fully fledged dynamical overlap or domain-wall study essentially at the costs of a staggered run.

## Acknowledgments

S.D. and U.W. would like to acknowledge stimulating discussions with Karl Jansen, Ch.H. with Laurent Lellouch and Leonardo Giusti. S.D. is supported by DFG in SFB/TR-9, Ch.H. is supported by EU grant HPMF-CT-2001-01468.

## References

- [1] C.T.H. Davies *et al.* [HPQCD Collaboration], hep-lat/0304004.
- [2] K. Jansen, Nucl. Phys. Proc. Suppl. **129**, 3 (2004) [hep-lat/0311039].
- [3] T. DeGrand, Int. J. Mod. Phys. A **19**, 1337 (2004) [hep-ph/0312241].
- [4] L. Susskind, Phys. Rev. D **16**, 3031 (1977).
- [5] R. Narayanan and H. Neuberger, Nucl. Phys. B **412**, 574 (1994) [hep-lat/9307006].  
R. Narayanan and H. Neuberger, Nucl. Phys. B **443**, 305 (1995) [hep-th/9411108]. H. Neuberger, Phys. Lett. B **417**, 141 (1998) [hep-lat/9707022]. H. Neuberger, Phys. Lett. B **427**, 353 (1998) [hep-lat/9801031].
- [6] D.B. Kaplan, Phys. Lett. B **288**, 342 (1992) [hep-lat/9206013]. Y. Shamir, Nucl. Phys. B **406**, 90 (1993) [hep-lat/9303005].
- [7] P. Hasenfratz and F. Niedermayer, Nucl. Phys. B **414**, 785 (1994) [hep-lat/9308004]. T. DeGrand, A. Hasenfratz, P. Hasenfratz and F. Niedermayer, Nucl. Phys. B **454**, 587 (1995) [hep-lat/9506030]. U.J. Wiese, Phys. Lett. B **315**, 417 (1993) [hep-lat/9306003]. W. Bietenholz and U.J. Wiese, Nucl. Phys. B **464**, 319 (1996) [hep-lat/9510026].
- [8] P.H. Ginsparg and K.G. Wilson, Phys. Rev. D **25**, 2649 (1982).
- [9] M. Lüscher, Phys. Lett. B **428**, 342 (1998) [hep-lat/9802011].
- [10] T. Blum *et al.*, Phys. Rev. D **55**, 1133 (1997) [hep-lat/9609036]. G.P. Lepage, Phys. Rev. D **59**, 074502 (1999) [hep-lat/9809157]. K. Orginos, D. Toussaint and R.L. Sugar [MILC Collaboration], Phys. Rev. D **60**, 054503 (1999) [hep-lat/9903032].
- [11] K. Symanzik, Nucl. Phys. B **226**, 187 (1983). K. Symanzik, Nucl. Phys. B **226**, 205 (1983).
- [12] P. Hernandez, K. Jansen and M. Lüscher, Nucl. Phys. B **552**, 363 (1999) [hep-lat/9808010].
- [13] T. DeGrand [MILC collaboration], Phys. Rev. D **63**, 034503 (2001) [hep-lat/0007046].
- [14] S. Dürr and Ch. Hoelbling, Phys. Rev. D **69**, 034503 (2004) [hep-lat/0311002].
- [15] B. Bunk, M. Della Morte, K. Jansen and F. Knechtli, hep-lat/0403022.
- [16] M. Albanese *et al.* [APE Collaboration], Phys. Lett. B **192**, 163 (1987).

- [17] A. Hasenfratz and F. Knechtli, Phys. Rev. D **64**, 034504 (2001) [hep-lat/0103029].  
A. Hasenfratz, R. Hoffmann and F. Knechtli, Nucl. Phys. Proc. Suppl. **106**, 418 (2002) [hep-lat/0110168].
- [18] J.E. Kiskis, R. Narayanan and H. Neuberger, Phys. Lett. B **574**, 65 (2003) [hep-lat/0308033].
- [19] E. Follana, A. Hart and C.T.H. Davies, hep-lat/0406010.
- [20] The Gauge Connection at the US National Energy Research Scientific Computing Center, <http://qcd.nersc.gov/>
- [21] F.R. Brown *et al.*, Phys. Rev. Lett. **67**, 1062 (1991).
- [22] T. Kalkreuter and H. Simma, Comput. Phys. Commun. **93**, 33 (1996) [hep-lat/9507023].
- [23] R. Sommer, Nucl. Phys. B **411**, 839 (1994) [hep-lat/9310022].
- [24] M. Guagnelli, R. Sommer and H. Wittig [ALPHA collaboration], Nucl. Phys. B **535**, 389 (1998) [hep-lat/9806005].
- [25] P.H. Damgaard, U.M. Heller, R. Niclasen and K. Rummukainen, Phys. Rev. D **61**, 014501 (2000) [hep-lat/9907019].
- [26] L. Giusti, M. Lüscher, P. Weisz and H. Wittig, JHEP **0311**, 023 (2003) [hep-lat/0309189].
- [27] P. Hasenfratz, S. Hauswirth, T. Jörg, F. Niedermayer and K. Holland, Nucl. Phys. B **643**, 280 (2002) [hep-lat/0205010].
- [28] K. Jansen and K.-I. Nagai, JHEP **0312** (2003) 038 [hep-lat/0305009].